

LA-UR-01-353

Predicting total reaction cross sections for nucleon-nucleus scattering

P. K. Deb¹, K. Amos¹, S. Karataglidis², M. B. Chadwick², and D. G. Madland²

¹*School of Physics, University of Melbourne, Parkville, Victoria, Australia, 3010*

²*Theoretical Division, Los Alamos National Laboratory, Los Alamos, New Mexico, 87545*

(April 26, 2024)

Abstract

Nucleon total reaction and neutron total cross sections to 300 MeV for ^{12}C and ^{208}Pb , and for 65 MeV scattering spanning the mass range, are predicted using coordinate space optical potentials formed by full folding of effective nucleon-nucleon interactions with realistic nuclear ground state densities. Good to excellent agreement is found with existing data.

Typeset using REVTeX

In this letter we present the first predictions of integral observables for both proton and neutron scattering for energies to 300 MeV (from ^{12}C and ^{208}Pb specifically) using, without approximation, complex, nonlocal, coordinate-space optical potentials formed by full folding realistic, effective, nucleon-nucleon (NN) interactions with density matrices (hereafter called densities) specified from credible models of the structure of the targets. That predictions agree with observation forebodes well for the use of such calculated values as are needed in a number of fields of study; some of quite current interest.

An example of such a topical study concerns the transmutation of long-lived radioactive waste into shorter-lived products, which together with energy production, uses accelerator-driven systems (ADS). These systems are being designed in the US, Europe, and Japan, for providing an intense neutron source to a subcritical reactor. The technology takes advantage of spallation reactions [1] in a thick high- Z target (such as Pb or Bi), where an intermediate-energy proton beam induces nuclear reactions and the secondary nuclear products, particularly lower-energy neutrons and protons [2], in turn induce further nuclear reactions in a cascade process. The total reaction cross section plays a particularly important role since the secondary particle production cross sections are directly proportional to this quantity, which often are inputs to intranuclear cascade simulations that guide ADS design.

In more basic science, the total reaction cross section is an important ingredient to a number of problems in astrophysics, such as nucleosynthesis in the early universe and for aspects of stellar evolution. The density distribution of neutrons in nuclei is far less well known than that of protons. By considering the integral observables of both proton and neutron scattering from a given nucleus one may seek direct information on the neutron root-mean-square radius; a property sought in parity-violating electron scattering experiments [3].

But most nucleon-nucleus (NA) total reaction cross sections have not been measured. Thus we must have a reliable method for their prediction. The usual vehicle for specifying NA total reaction cross sections has been the NA optical potential; a potential most commonly taken as a local parametrized function, usually of Woods-Saxon type. However, it has long been known that the optical potential must be nonlocal and markedly so, although it has been assumed also that the energy dependence of the customary (phenomenological) model accounts for that. Of more concern is that the phenomenological approach is not truly predictive. The parameter values chosen, while they may be set from a global survey of data analyses, are subject to uncertainties and ambiguities leading, for example, to different values of the total reaction cross section while yielding comparable elastic angular distributions.

We consider a predictive theory of NA scattering to be one that is *direct* for which all quantities required are defined *a priori*, with no *a posteriori* adjustment of results. With the nucleus viewed as a system of A nucleons, NA scattering is determined by an optical potential formed by a folding process. That folding we choose to be of realistic interactions of the projectile with each and every nucleon constituting the ground state target density. Such microscopic approaches defining the NA optical potential have been quite successful in predicting angle-dependent observables of elastic scattering [4]. In the coordinate space approach, and for analyses that use the DWBA98 programs [5], the projectile-target nucleon interaction is not only complex but also energy and density dependent. We have used that program herein to calculate all integral cross sections with realistic effective interac-

tions folded with reasonable descriptions of the densities of nuclei to give credible optical potentials. Using those optical potentials, differential cross sections and spin observables, for proton scattering at many energies in the range 40 to 800 MeV (65 and 200 MeV in particular) and from diverse targets ranging from ${}^3\text{He}$ to ${}^{238}\text{U}$ have been predicted and found to agree very well with measured values. The (nonlocal) optical potentials are complex and energy dependent; properties that arise from mapping the effective interactions to NN g matrices that are solutions of the Brueckner-Bethe-Goldstone (BBG) equations for nuclear matter. Details of the specifications of the effective interactions, of the folding process that gives the optical potential, and of the successful predictions of differential cross sections and analyzing powers from the scattering of protons at diverse energies and from diverse mass targets, have been recently summarized [4].

Formally, the nonlocal optical potentials can be written

$$\begin{aligned} U(\vec{r}_1, \vec{r}_2; E) &= \sum_n \zeta_n \left\{ \delta(\vec{r}_1 - \vec{r}_2) \int \varphi_n^*(\vec{s}) v_D(\vec{r}_{1s}) \varphi_n(\vec{s}) d^3s + \varphi_n^*(\vec{r}_1) v_{Ex}(\vec{r}_{12}) \varphi_n(\vec{r}_2) \right\} \\ &\Rightarrow U_D(\vec{r}_1; E) + U_{Ex}(\vec{r}_1, \vec{r}_2; E), \end{aligned} \quad (1)$$

where v_D , v_{Ex} are combinations of the components of the effective NN interactions, ζ_n are ground state one body density matrices (which often reduce to bound state shell occupancies), and $\varphi_n(\vec{r})$ are single nucleon bound states. All details and the prescription of solution of the associated nonlocal Schrödinger equations are given in the recent review [4].

The results to be discussed herein have been obtained by solving the actual nonlocal Schrödinger equations defined with potentials as given by Eq. (1). For the present calculations, the effective NN interactions have been defined by their mapping to the BBG g matrices of the BonnB NN interaction [6]. When those effective interactions are folded with the appropriate ground state target densities we obtain the “g-folding” optical potentials. Calculations have also been made using solely the free NN t matrix in this prescription, the results of which are “ t -folding” optical potentials.

The specification of the nuclear ground state density is taken from a given nucleon-based model of structure. For the light nuclei ($A \leq 16$) we use complete (no core) multi- $\hbar\omega$ shell models [4]. For ${}^{12}\text{C}$, specifically, we have constructed a complete $(0+2)\hbar\omega$ shell model using the WBT interaction of Warburton and Brown [7]. For ${}^{208}\text{Pb}$, the other nucleus under investigation, we have used both a simple packed shell model with an oscillator specified by an $A^{1/3}$ rule and a Skyrme-Hartree-Fock (SHF) specification [3] of the ground state.

The first objective of specifying the optical potentials is to define the S matrix, or equivalently the (complex) phase shifts $\delta_l^\pm(k)$ which relate by

$$S_l^\pm \equiv S_l^\pm(k) = e^{2i\delta_l^\pm(k)} = \eta_l^\pm(k) e^{2i\Re[\delta_l^\pm(k)]} \quad (2)$$

where

$$\eta_l^\pm \equiv \eta_l^\pm(k) = |S_l^\pm(k)| = e^{-2\Im[\delta_l^\pm(k)]}. \quad (3)$$

In terms of these and with $E \propto k^2$, the elastic and total reaction (absorption) cross sections are given by

$$\begin{aligned}\sigma_{\text{el}}(E) &= \frac{\pi}{k^2} \sum_{l=0}^{\infty} \left\{ (l+1) \left| S_l^+ - 1 \right|^2 + l \left| S_l^- - 1 \right|^2 \right\} , \\ \sigma_R(E) &= \frac{\pi}{k^2} \sum_{l=0}^{\infty} \left\{ (l+1) \left[1 - (\eta_l^+)^2 \right] + l \left[1 - (\eta_l^-)^2 \right] \right\} ,\end{aligned}\quad (4)$$

respectively. The total cross section, $\sigma_{\text{TOT}}(E)$, is the sum of these two cross sections.

In Fig. 1, proton total reaction cross-section data at 65.5 MeV [8] from a diverse set of nuclei are compared with our predictions obtained using both the g and t folding optical potentials. Quite clearly, with large complete space shell model densities [4] for masses 9 to 12, complete $0\hbar\omega$ densities for sd -shell nuclei to ^{40}Ca , packed structure models for the Ni and Sn isotopes, and the SHF model for ^{208}Pb , the medium modifications generating the g folding potentials are essential to give agreement with experiment.

There are a number of small breaks in the mass variation of the g folding results from a smooth trend. These reflect density variations with isotopes created even by the simple $0\hbar\omega$ model and which influence how specifics of the effective interactions are selected in folding. Such variations have lesser influence in defining the t -folding optical potentials; hence the smoother variation with mass of the t -folding total reaction cross sections. However, the t -folding results consistently overestimate the data.

The total reaction cross sections for proton and neutron scattering from ^{12}C up to 300 MeV are presented in sections (a) and (b), respectively, of Fig. 2. The proton data have been obtained from many experiments [8,9]. The neutron data were obtained from References [10–13]. The solid curves are our g -folding model predictions. Clearly, with the exception of the data below 20 MeV and of two data points at 61 and 77 MeV, our predictions of the proton total reaction cross sections are quite good. The mismatch below 20 MeV does not vitiate our method of analysis for higher energies. The spectrum of ^{12}C , and also of the compound mass-13 system, has many discrete states and so nucleon scattering will reflect effects of (discrete) thresholds, isolated compound nuclear resonances, etc. Our first order folding model of potential scattering has not been designed to accommodate such specific structures and processes. The exceptional data points also should be discounted. Not only do they differ markedly from the trend of other data in the vicinity but also there are data points at 60.8 and 65.5 MeV that conflict with them. The neutron total reaction cross-section data vary with energy as do our g folding predictions but we overestimate the extracted experimental values by some 10-20%. However, the neutron total reaction cross section data are difficult to measure and further judgement of these results should be held in abeyance until we consider the neutron total cross sections.

The total reaction cross sections for proton and neutron scattering from ^{208}Pb are displayed in Figs. 3(a) and 3(b), respectively. The proton data were taken from references [8] and [9] and the neutron data from references [11–15]. We compare those data again with the predictions obtained using two sets of g folding optical potentials. In all cases, at each energy, the same effective interaction appropriate for that energy has been used to give the optical potentials. The dashed curves are predictions one obtains when simple $0\hbar\omega$ shell model densities are used in the folding process, while the solid curves depict our predictions found by folding with the SHF densities. The differences between these predictions are not large, but in comparison with the data, the SHF model is preferred. Both calculations slightly underestimate the data in the range of energies 10 to 40 MeV. In contrast, our

results overestimate most of the neutron total reaction cross section data. But as with the ^{12}C case, any judgement of the neutron data mismatch should await consideration of the total scattering cross sections.

However, note that proton (neutron) scattering from nuclei are most influenced by the folding with the neutron (proton) densities given the preponderance of the isoscalar 3S_1 NN interaction in such foldings. Also, with increasing energy, the central attributes of the optical potentials gain in importance in determining the scattering phase shifts and hence the total reaction cross sections. At low energies, not only do relatively few partial waves contribute to the calculations, but also the centrifugal barrier more effectively screens the waves from the influence of the bulk of the optical potential, hence lower energy scattering tends to be a surface effect. Thus, as the SHF and $0\hbar\omega$ model densities differ most noticeably in the nuclear interior, the proton scattering cross sections found with these two model densities differ by about 100 mb for energies above 100 MeV but are more equivalent at lower energies. The discrepancy with data at lower energies then indicates that the surface distributions of neutrons in ^{208}Pb are even more extended than given by either model.

The total scattering cross sections of neutrons from ^{12}C and ^{208}Pb are displayed in Figs. 4(a) and 4(b), respectively. The data shown therein are those of Finlay *et al.* [16] and they are compared with our g folding optical potential predictions. Overall, our predictions are in good agreement with the data and the SHF result in ^{208}Pb gives a better reproduction of the Ramsauer diffraction structure in the 30 to 200 MeV region in comparison to the recent semi-microscopic optical model result [17]. Noticeably, for both nuclei, there is no overestimation of the data in the 50 to 100 MeV region in contrast to the total reaction cross-section comparisons. The g folding optical potentials lead also to excellent reproductions of differential cross-section data [4] with implications that the total elastic cross sections are well predicted. Thus for neutron scattering, we are confident that our total reaction cross sections are also realistic.

We have demonstrated that our g folding optical potential procedure gives integral observables in good agreement with existing data. Particularly, we conclude that the low energy data (typically to 60 MeV) are sensitive to the surface density properties and of the neutrons for the heavy nuclei in particular. At higher energies, the surface densities remain important, but it is the bulk density that largely determines the scattering. As a consequence, an analysis of proton and neutron integral cross sections with energy can shed light on the neutron density distribution in nuclei.

This work was supported by a grant from the Australian Research Council and also by DOE Contract no. W-7405-ENG-36.

REFERENCES

- [1] W. Wlazlo, *et al.*, Phys. Rev. Lett. **84**, 5736 (2000).
- [2] X. Ledoux, *et al.*, Phys. Rev. Lett. **82**, 4412 (1999).
- [3] B. A. Brown, Phys. Rev. Lett. **85**, 5296 (2000).
- [4] K. Amos, P. J. Dortmans, H. V. von Geramb, S. Karataglidis, and J. Raynal, Adv. in Nucl. Phys. **25**, 275 (2000).
- [5] J. Raynal, *computer code DWBA98* (1999), (NEA 1209/05).
- [6] R. Machleidt, Adv. in Nucl. Phys. **19**, 189 (1989).
- [7] E. K. Warburton and B. A. Brown, Phys. Rev. C **46**, 923 (1992).
- [8] A. Ingemarsson, J. Nyberg, P. U. Renberg, O. Sundberg, R. F. Carlson, A. Auce, R. Johansson, G. Tibell, B. C. Clark, L. K. Kerr, *et al.*, Nucl. Phys. **A653**, 341 (1999).
- [9] R. F. Carlson, Atom. Data and Nucl. Data Tables **63**, 93 (1996).
- [10] C. Zanelli, P. Urone, J. Romero, F. Brady, M. Johnson, G. Needham, J. Ullmann, and D. Johnson, Phys. Rev. C **23**, 1015 (1981).
- [11] M. H. MacGregor, W. P. Ball, and R. Booth, Phys. Rev. **111**, 1155 (1958).
- [12] R. G. P. Voss and R. Wilson, Proc. Roy. Soc. A **236**, 52 (1956).
- [13] J. Dejuren and N. Knable, Phys. Rev. **77**, 606 (1950).
- [14] T. W. Bonner and J. H. Slattery, Phys. Rev. **113**, 1088 (1959).
- [15] J. G. Degtjarev and V. G. Nadtchij, Sov. J. Nucl. Phys. **11**, 1043 (1962).
- [16] R. W. Finlay, W. P. Abfalterer, G. Fink, E. Montei, T. Adami, P. W. Lisowski, G. L. Morgan, and R. C. Haight, Phys. Rev. C **47**, 237 (1993).
- [17] E. Bauge, J. P. Delaroche, and M. Girod, Phys. Rev. C **58**, 1118 (1998).

FIGURES

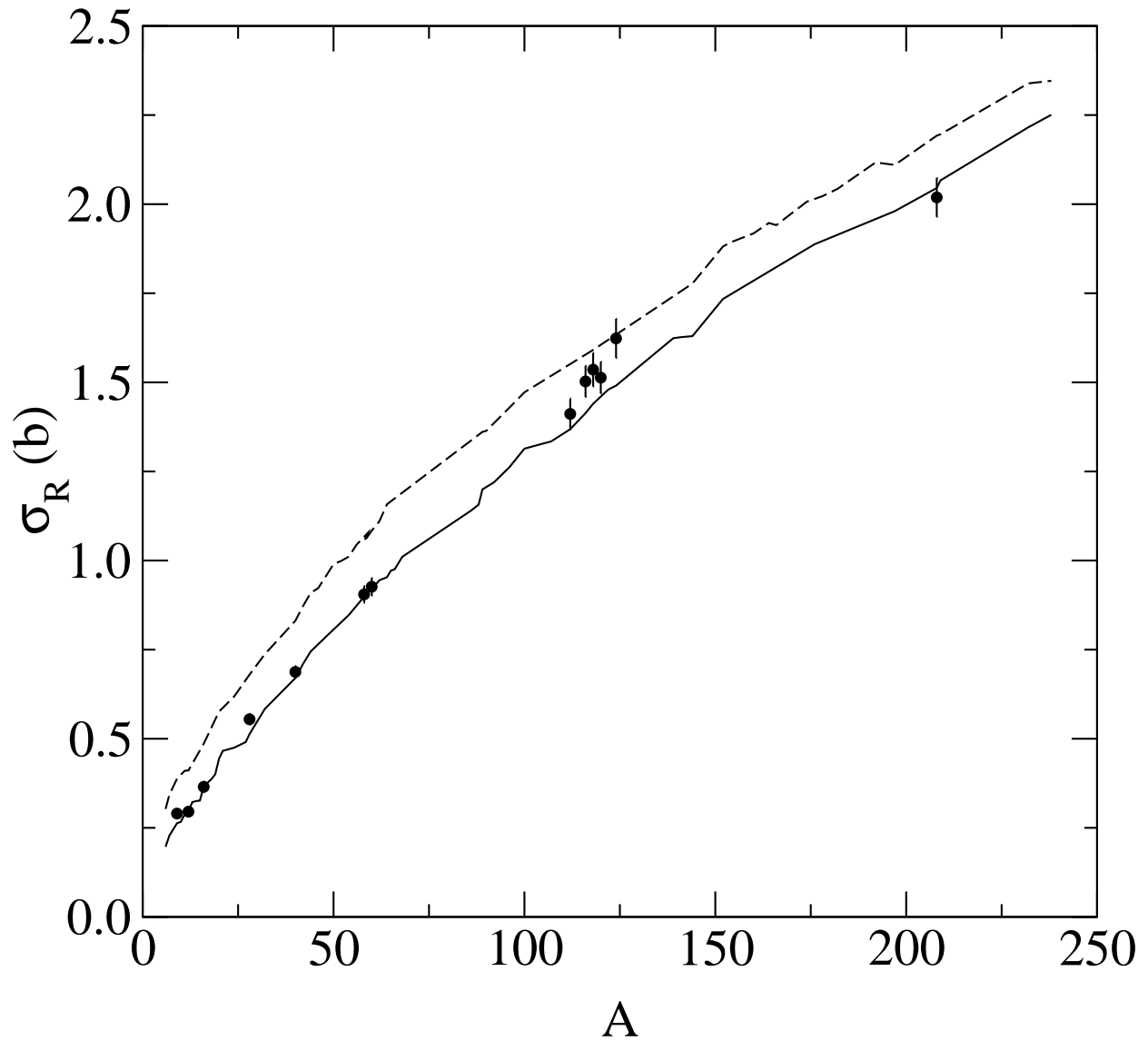


FIG. 1. Total reaction cross section at 65.5 MeV as a function of target mass. The g -folding (solid line) and t -folding (dashed line) results are compared to the data of Ingemarsson [8].

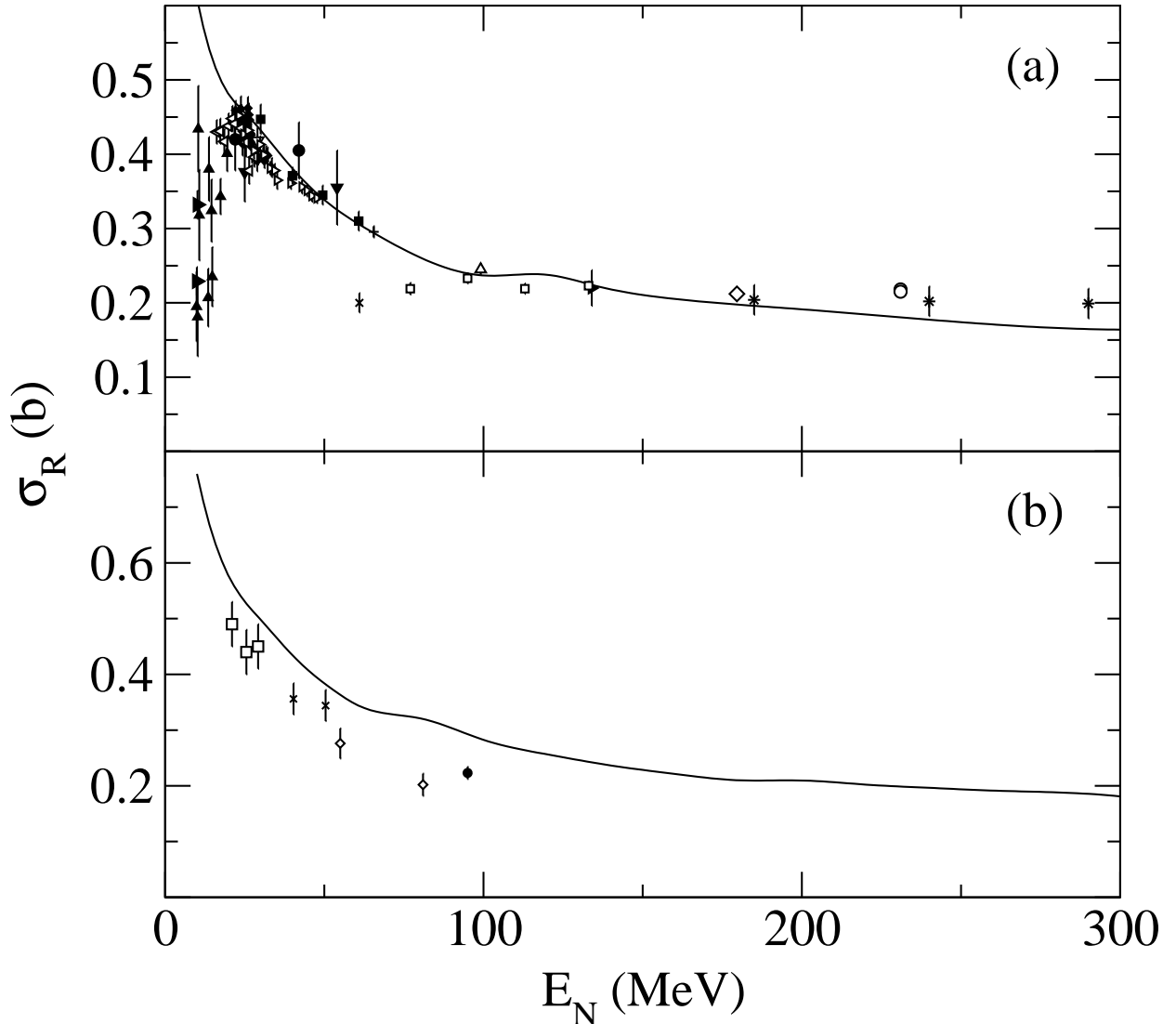


FIG. 2. Energy dependence of the total reaction cross section for the scattering of nucleons from ^{12}C . In (a), the results for the scattering of protons are compared with data taken from many sources as listed in the compilation by Carlson [9], and from more recent data of Ingemarsson *et al.* [8]. In (b), the results for the scattering of neutrons are compared with the data of Refs. [10] (crosses), [11] (squares), [12] (diamonds), and [13] (circle).

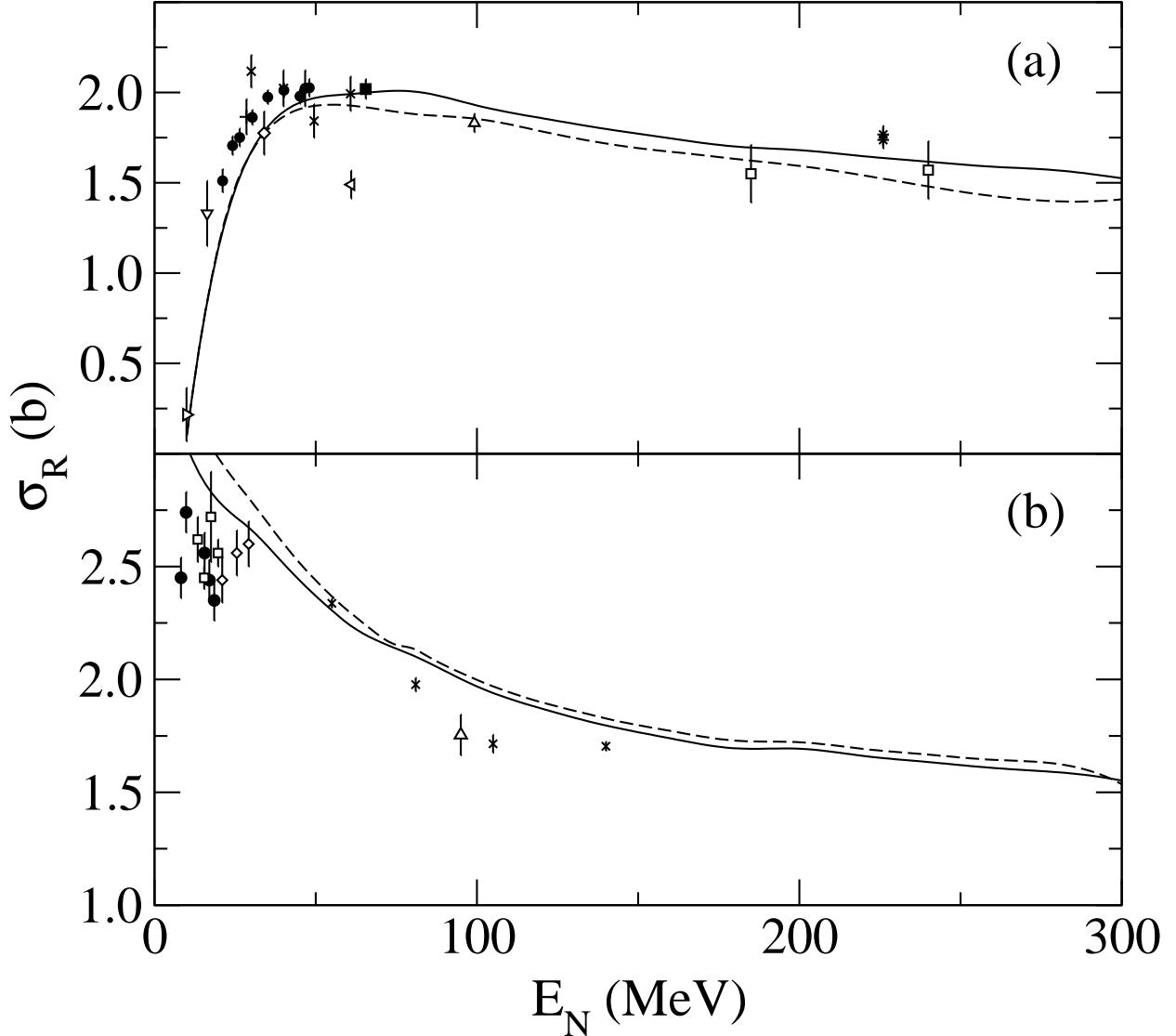


FIG. 3. As for Fig. 2 but for the scattering of nucleons from ^{208}Pb . The data for the neutron total reaction cross sections were from Refs. [11] (diamonds), [12] (crosses), [13] (triangle), [14] (circles), and [15] (squares). The additional dashed curves were obtained using simple $0\hbar\omega$ shell model densities.

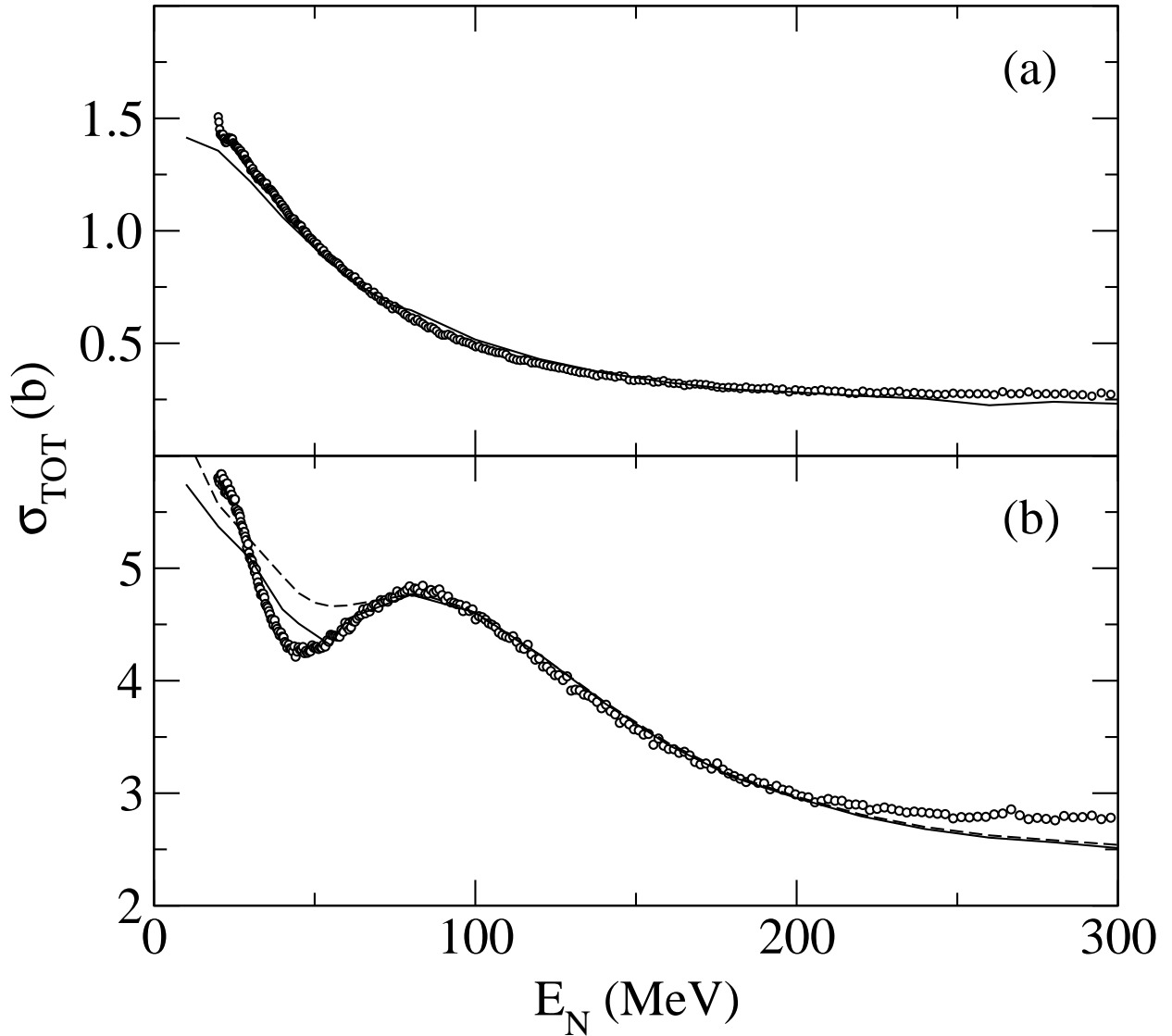


FIG. 4. Total cross section for the scattering of neutrons from ^{12}C (a) and ^{208}Pb (b). The data of Finlay *et al.* [16] are compared to the results of the g folding calculations. The solid and dashed curves are as for Fig. 3.